Supporting Information

Modulated Oxygen Vacancy in Europia Clusters/Black Phosphorus Induced Signal Amplification for Efficient Chemiluminescence Sensing

Hui Gong,[a] Dayang Zhao,[a] Yu Zhou,[a] Yuxian Zhou,[a] Jing Gou,[a] Houjing Liu,[a]*

[a.] *College of Chemistry & Chemical Engineering, Guizhou University, Guiyang 550025, China.*

Corresponding Author. Email: hjliu3@gzu.edu.cn

Chemicals and Reagents. Red phosphorus, iodine (I_2), and tin (Sn) were all obtained from Kelong Chemical Factory (Chengdu, China). Europium (III) trifluoromesulfonate and NaClO were bought from Sigma-Aldrich Company (Shanghai, China). N-methyl-2-pyrrolidinone (NMP) and N, N-dimethylformamide (DMF) from KeYi regent company (Guiyang, China). Other reagents were purchased from TaiTan Chemical Reagent Company (Shanghai, China). All experimental aqueous solutions were prepared using ultrapure water, which was treated by a specialized instrument (a Milli-QULUPURE, Chengdu, China).

Experimental apparatus. All the CL experiments were measured on the Ultra-weak chemiluminescence instrument (BPCL-2-TGC, Guangzhou, China). UV-vis absorption spectrum was recorded on the Shimadzu UV-2700 ultraviolet-visible spectrophotometer (Shimadzu, China). VERTEX70 infrared spectrometer (Brooks, Germany) was used to record Fourier transform infrared spectroscopy (FT-IR) spectra of Eu_2O_3/BPQDs. The size and morphology of Eu_2O_3/BPQDs were recorded by Tecnai G2 F20 S-TWIN (200KV) field emission transmission electron microscope (TEM). All fluorescence spectra were obtained from a fluorescence spectrophotometer (Varian, USA). The X-ray photoelectron spectroscopy (XPS) spectra of material were collected with Thermo Fisher (ESCA Lab 250Xi, USA). Raman spectrum was measured on a Lab Ram HR800 Raman spectroscopy (Horiba Jobin Yvon Inc. France), we used a Bruker E-500 instrument (microwave power 12.72 mW,

microwave frequency 9.77 GHz, modulation frequency 100 kHz, and sweep width 3480 G) to carry out the EPR measurements.

Synthesis of Eu_2O_3/BPQDs. Eu_2O_3/BPQDs were fabricated via solvothermal treatment of bulk BP with saturated NaOH in N-methyl-2-pyrrolidone (NMP) solution. The synthetic process of bulk BP is shown in the ESI†. Usually, the synthesis methods of BP-based QDs include ultrasonic stripping, electrochemical stripping, solvent-thermal synthesis and so on. In this paper, Eu_2O_3/BPQDs were synthesized using bath oiling. The specific operations are as follows: 10 mg BP was ground with NMP for a period of time to form a uniform solution. The obtained solution was transferred to a 250 mL three-neck flask with round bottom, and 100 mg NaOH, 100 mL NMP and 5 mg Europium (III) tri-fluoromesulfonate were added. Then, the solution was refluxed in 140 ℃ oil bath for 6 hours under nitrogen condition, which was used to remove dissolved oxygen. After the reaction was cooled, the supernatant was collected by centrifugation at 8000 rpm for further treatment. To remove NMP solvent, the above solution was disposed by rotary evaporation and centrifugation at high speed (15000 rpm for 20 min). Finally, the acquired precipitates were dried and kept in vacuum for further use. And when being used, the resulted product was dissolved into DMF solvent to form a solution containing Eu_2O_3/BPQDs for later experiments.

Note: The mass of the dried precipitates is 1.02 mg, the synthesis yield of Eu_2O_3/BPQDs [(1.02/15) %] was 6.8%.

CL experiment. All CL signals were obtained by static injection. The reaction quartz cell containing the sample was set close to photomultiplier tube. For Eu_2O_3/BPQDs-ClO^- system, the specific CL experiment operation is as follows: a mixture of 800 μL Eu_2O_3/BPQDs solution was placed in a quartz cell, and 200 μL ClO^- solution was rapidly injected into the quartz cell by a peristaltic pump to react with the above solution, while the CL signals were recorded by BPCL. The CL emission was detected by the voltage of the PMT (0.8 kV) with an interval of 0.01 s for data acquisition and the temperature was 25℃. Additionally, to ensure the reliability of dates, more than three replicate CL measurements were performed for each point and all date points were collected in the same day. Conditions: The volumes of BP nanosheet, BPQDs, Eu_2O_3/BPQDs were all 800 μL, and the volumes of anions, cations, scavengers were all 200 μL. The concentrations of Eu_2O_3/BPQDs and ClO^- were 0.04 mg/mL, 0.02 mol/L.

CL quantum yields of Eu_2O_3/BPQDs-ClO^- system. The chemiluminescence quantum yield (QY) values of the Eu_2O_3/BPQDs-ClO^- system was determined by using the luminol-H_2O_2 system as the standard with a known CL QY of 1.14×10^{-2} E/mol at pH=11.6 (0.1 M K_2CO_3) according to the literature. [1] Briefly, a solution of Eu_2O_3/BPQDs (0.04 mg mL^{-1} 800 μL) was placed in a tube, and then Sodium hypochlorite (0.002 M, 200 μL) was added to the solution. CL dynamic curves of the mixture was measured until the CL intensity reduced to 1% of the highest value, by using a CL analyzer. The voltage of PMT was 0.8 kV for the CL detection and signal acquisition time of the CL analyzer was set at 0.1 s at intensity mode. The same procedure was carried out with a mixture of luminol (1 μM, 100 μL, in 0.1 M K_2CO_3) and hydrogen peroxide (100 μL, 1 mM). The CL QY value of Eu_2O_3/BPQDs-ClO^- was relatively calculated from the integrated areas under curves according to the following equation:

$$\phi = \phi_{\text{lum}} \times \frac{I}{I_{lum}} \times \frac{n^2}{n_{lum}{}^2} \times \frac{[Luminol]}{[Eu_2O_3/BPQDs]}$$

I is the total number of photons obtained by integration of CL dynamic curves under time until the CL intensity reduced to 1% of the highest value，where ϕ was the quantum yield, n was the refractive index of solvent, and [Luminol] and [Eu_2O_3/BPQDs] were concentrations.

Note: The CL quantum yield of Eu_2O_3/BPQDs-ClO^- was 3.01×10^{-8} einsteins/mol.

Atmospheric particulate samples collection and preparation. Guiyang, as an important industrial base in Guizhou Province, is located in a plateau mountain basin with typical karst landform features. Surrounded by mountains, it is characterized by calm winds, small winds and stable layer structure, which is not conductive to the diffusion and dilution of pollutants in the air. Therefore, the analysis of the distribution characteristics and sources of pollutants (such as: $PM_{2.5}$, PM_{10}) in Guiyang show significantly practical application. We acquired atmospheric particulates samples from a Zhenfeng Electric Power Investment Co., Ltd of Guiyang city, which is a typical fossil-fuel power station that produces atmosphere particulate pollution. Sampling points were arranged above the chimney mouth and samples were collected from four wind direction sites with east, west, north and south, in December 31, 2021. The resulting filters with atmospheric particulates were saved in a refrigerator at -18°C. The filter with atmospheric particulates was processed into small pieces. The obtained pieces were treated with an ultrasonic cleaner for 30 min at 500 W after mixing with proper amount of

deionized water. Then, the extracted mixture was filtered to remove the filter from the suspension and dried. Finally, a 0.22 μm hydrophilic membrane was used to suspension filter, and the obtained solution could be directly detected. We can calculate the concentration of atmospheric particulates based on the weight differences of the original and dried filter.

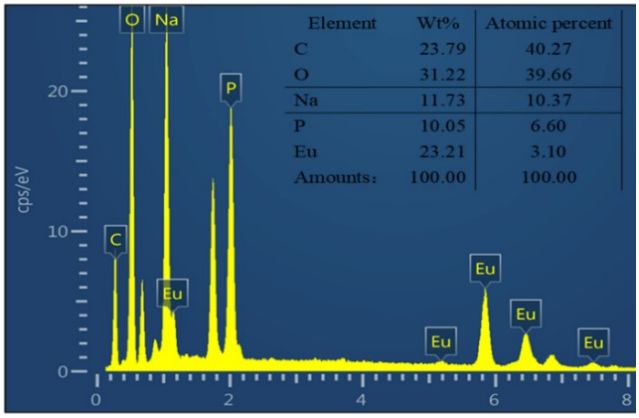

Figure 1s. The energy-dispersive X-ray spectroscopy (EDS) spectrum of Eu_2O_3/BPQDs.

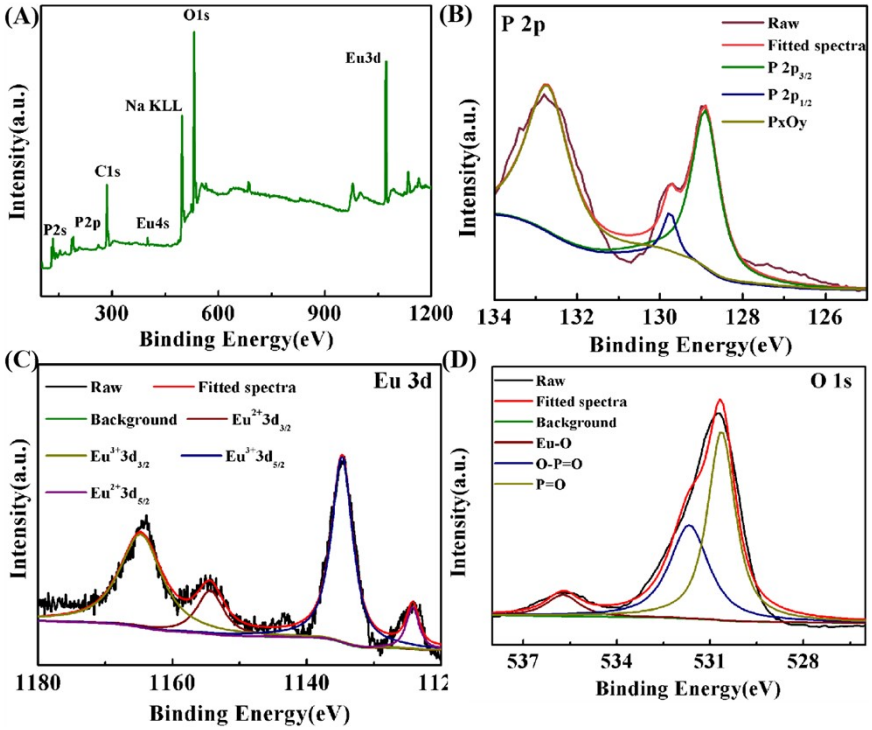

Figure 2s. (A) Survey XPS spectrum of Eu_2O_3/BPQDs. (B) and high-resolution XPS spectrum P 2p. (C) Eu 3d. (D) and O 1s from Eu_2O_3/BPQDs, respectively.

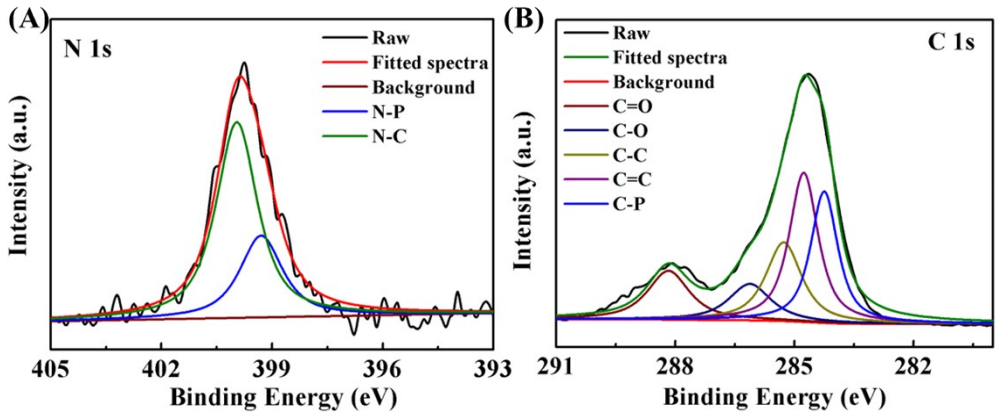

Figure 3s. High-resolution XPS spectrum of N 1s, and C 1s spectrum from Eu_2O_3/BPQDs, respectively.

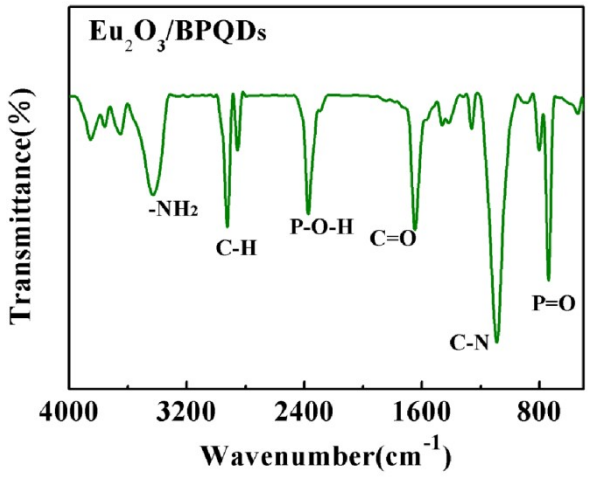

Figure 4s. The FT-IR analysis from Eu_2O_3/BPQDs.

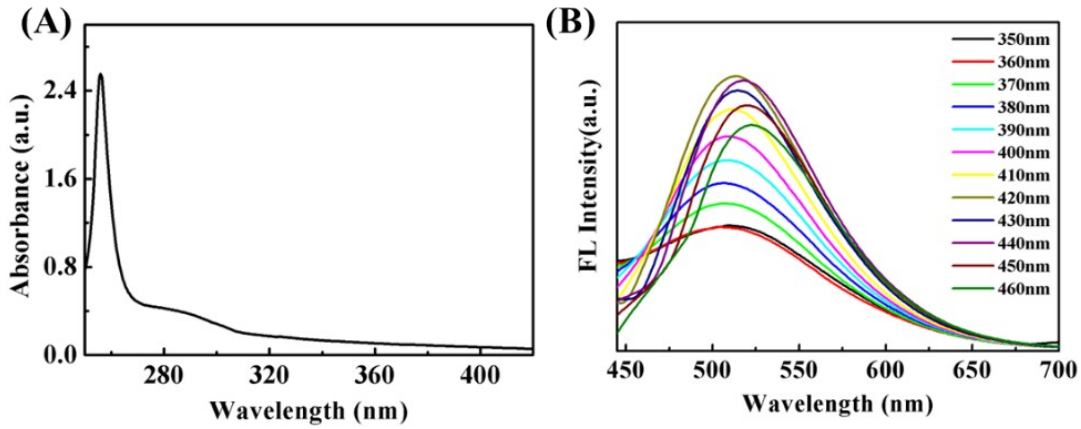

Figure 5s. UV−vis absorption and FL spectra of Eu_2O_3/BPQDs at different excitation wavelengths (legend: The concentration of BPQDs solution is 0.04 mg/mL).

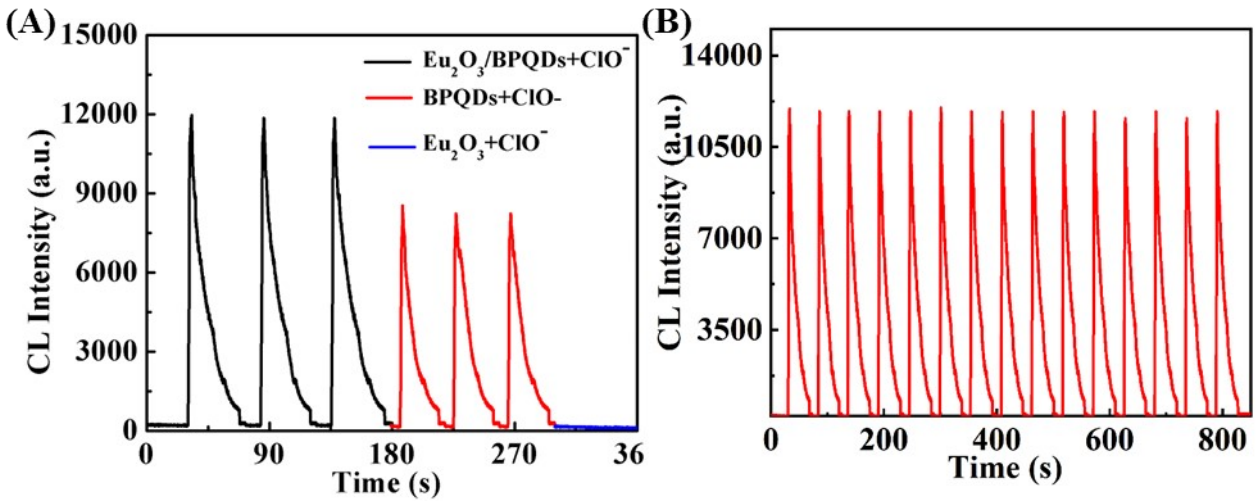

Figure 6s. (A) CL emission of ClO^- solution in the presence of Eu_2O_3/BPQDs (black), BPQDs (red), E_2O_3 (green) and CL emission of Eu_2O_3/BPQDs (blue), (B) Reproducible properties experiments of the Eu_2O_3/BPQDs – ClO^- system (Conditions: the concentrations of ClO^-, BPQDs, Eu_2O_3/BPQDs and Eu_2O_3 were 0.02 M, 0.04 mg/mL, 0.04 mg/mL, 0.04 mg/mL, respectively.).

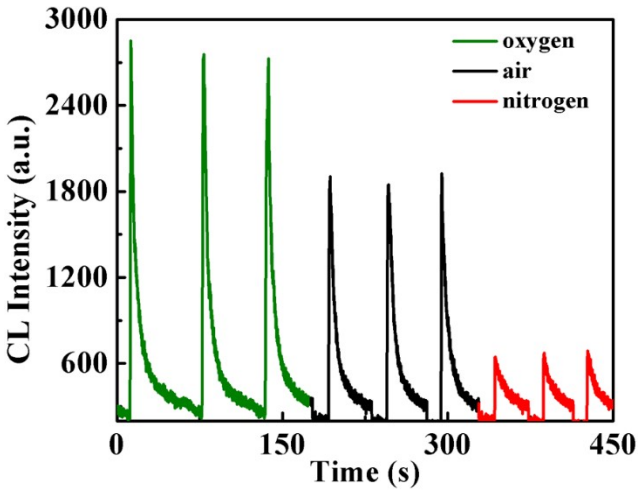

Figure 7s. The CL curves of Eu_2O_3/BPQDs-ClO^- system: the CL solution was bubbled with O_2 (green), N_2 (red) and air (black) for 30 min before mixing (Condition: ClO^- 0.01 M, Eu_2O_3/BPQDs 0.04 mg/mL).

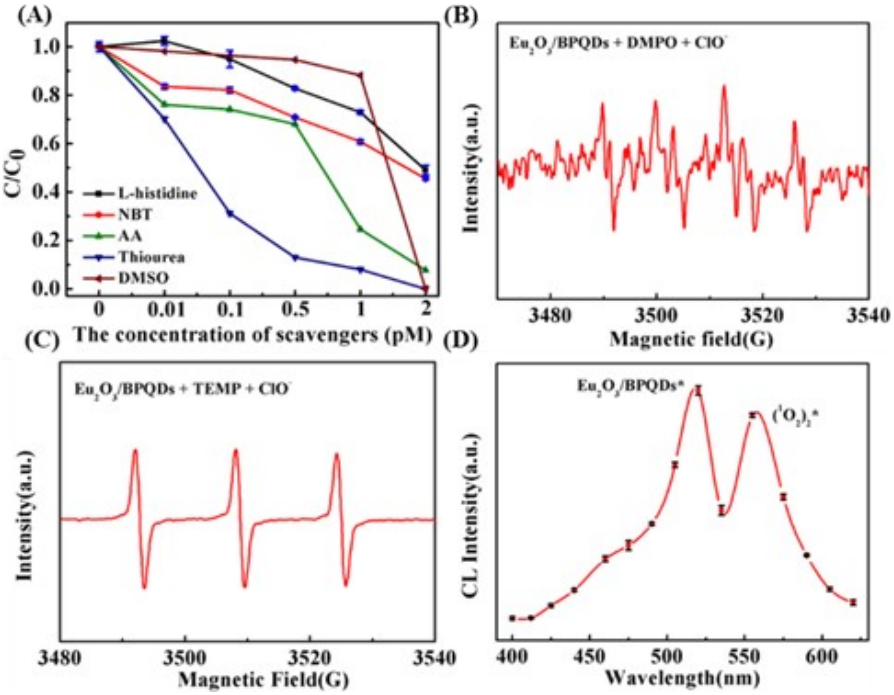

Figure 8s (A) The inhibition percentage of different scavengers on the CL intensity, (B-C) EPR spectra of $^{\bullet}OH$ and $^{1}O_2$ generating (D) The CL spectrum of Eu_2O_3/BPQDs-ClO^- system. Conditions: Eu_2O_3/BPQDs 0.04 mg mL^{-1}, DMPO 0.05 mol L^{-1}, TEMP 0.1 mol L^{-1}, and ClO^- 0.01 M.

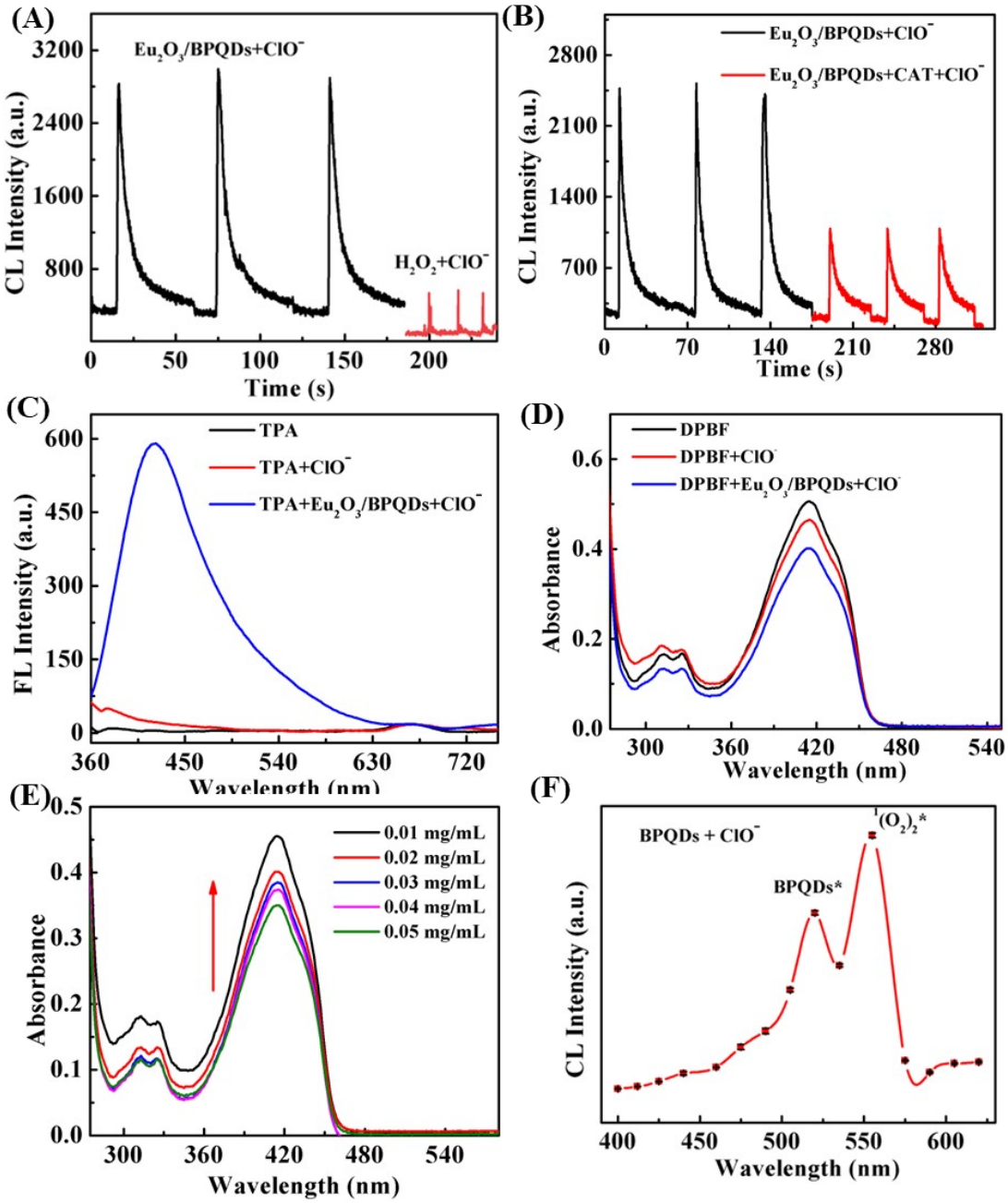

Figure 9s. (A) CL emission of ClO^- solution in the presence of H_2O_2 (red) and Eu_2O_3/BPQDs (black), (B) The effects of catalase (CAT) on CL intensity, (C) Fluorescence kinetic study on •OH generation in the Eu_2O_3/BPQDs-ClO^- CL system (The excitation wavelength was 330 nm), (D) Chemical trapping measurements of $^1O_2$: UV absorption spectra of DPBF, DPBF in ClO^-, and DPBF in the Eu_2O_3/BPQDs-ClO^- CL system, (E) Time-dependent absorption spectra of the DPBF in Eu_2O_3/BPQDs-ClO^- system, (F) The CL spectrum of BPQDs-ClO^- system (Conditions: the concentrations of ClO^-, H_2O_2, CAT, TPA, DPBF, Eu_2O_3/BPQDs and BPQDs were 0.16 M, 1 M, 2 mg mL^{-1}, 0.02 mg mL^{-1}, 0.02 mg mL^{-1}, 0.04 mg mL^{-1} and 0.1 mg mL^{-1}, respectively.).

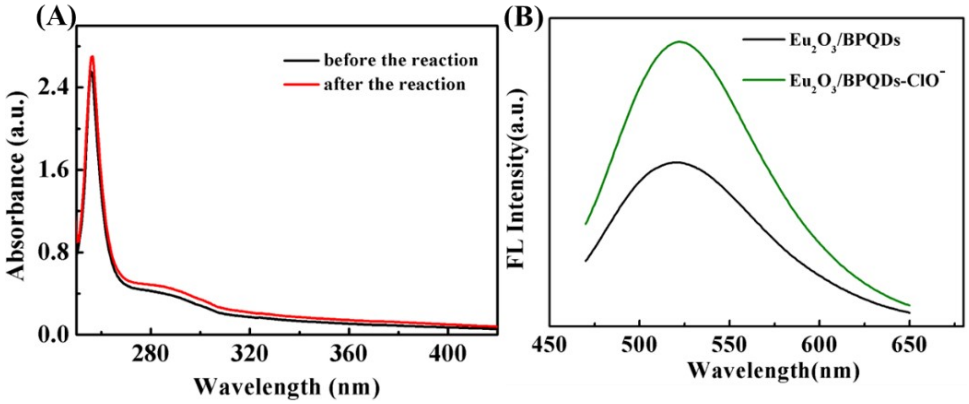

Figure 10s. UV−vis absorption and FL spectra of Eu_2O_3/BPQDs before and after reaction with ClO^- (Condition: ClO^- 0.01 M, Eu_2O_3/BPQDs 0.04 mg/mL).

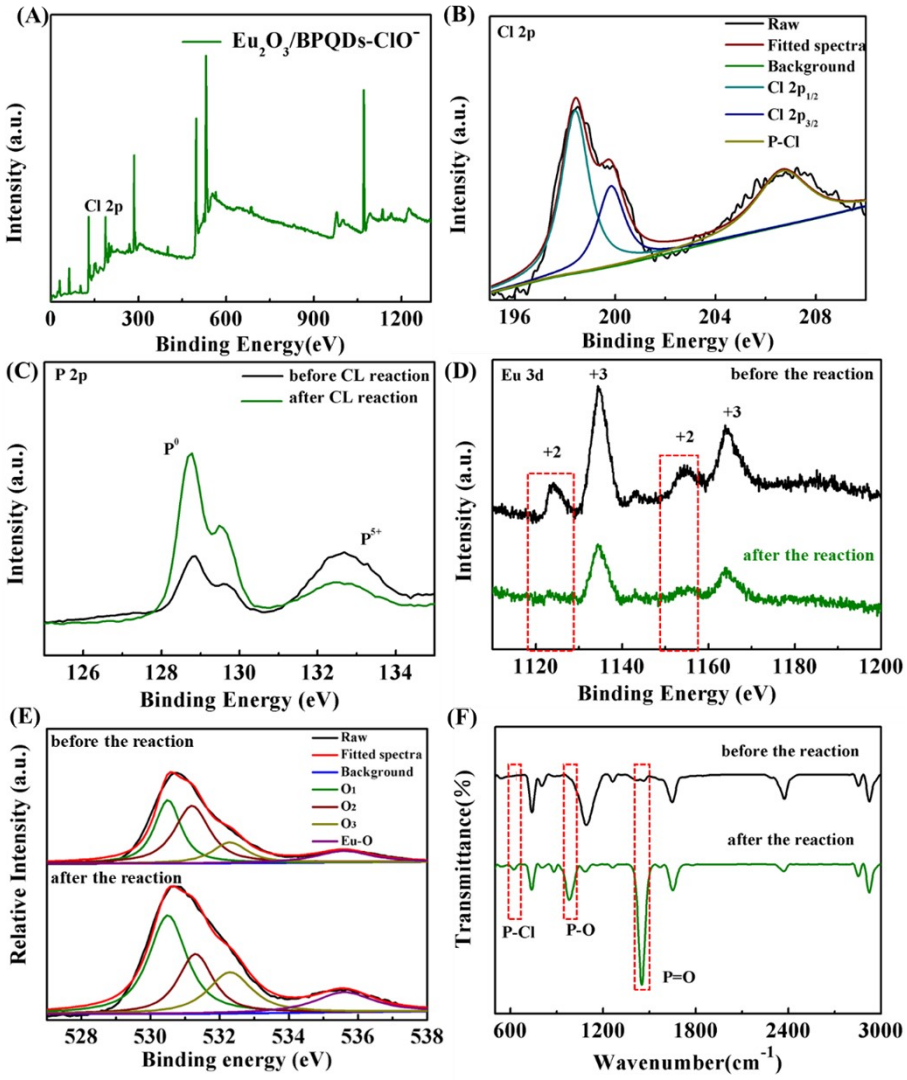

Figure 11s. (A) The full XPS spectrum of Eu_2O_3/BPQDs-ClO^- system. (B) High-resolution XPS spectrum Cl 2p (C-F) High-resolution XPS spectra P 2p peaks, Eu 3d peaks, O 1s peaks and FT-IR

analysis of Eu_2O_3/BPQDs before and after reaction with ClO^-.

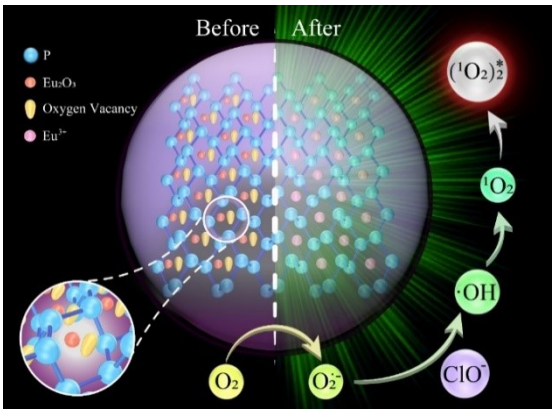

Figure 12s. Schematic illustration of the CL mechanism in the Eu_2O_3/BPQDs-ClO^- system.

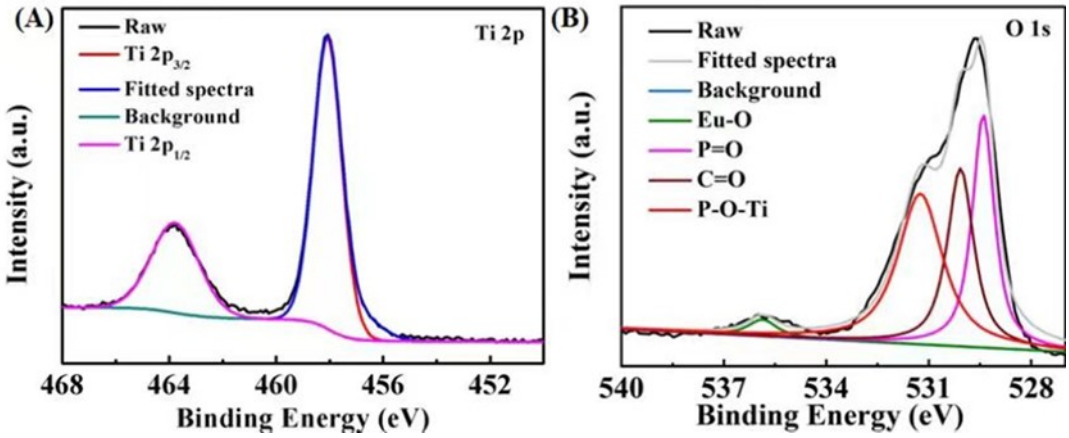

Figure 13s. High-resolution XPS spectrum of Ti 2p, and O 1s spectrum from Eu_2O_3/BPQDs-Ti^{4+}-ClO^- system, respectively.

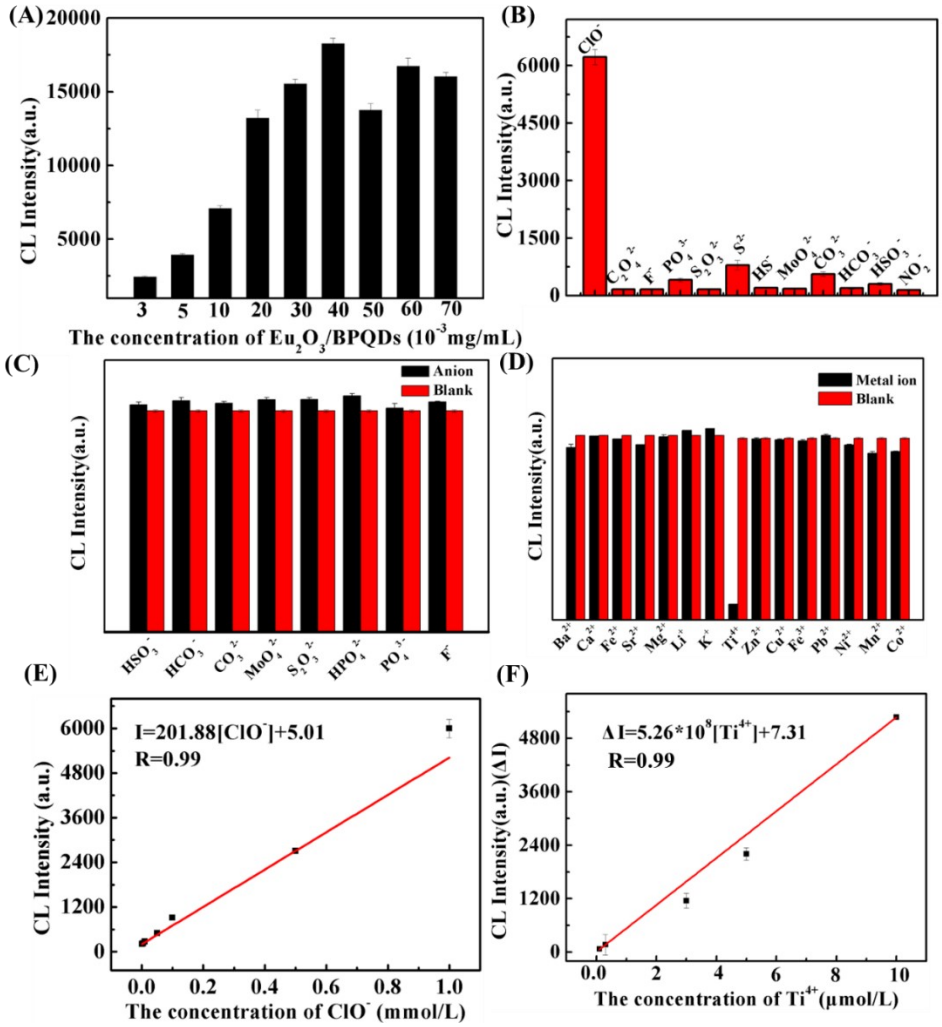

Figure 14s. Effects of (A) the concentration of Eu_2O_3/BPQDs on the CL intensity. (B) CL intensities of Eu_2O_3/BPQDs toward different anions. (C-D) The effects of anions and mental ions on CL intensity. (E-F) Linear relationship between CL intensities with different concentration of hypochlorite and titanium ions (Condition: The concentrations of anions and cations about interference experiment and selectivity experiment were all 0.0001 M).

Table S1. Comparisons of proposed method with recently reported strategies for ClO^- detection.

Detection probe	methods	Linear range	LOD	Samples	Reference
OR	UV–Vis	0–9 μM	0.20 μM	Water	[2]
NCDs	Electrochemiluminescence	0-40 μM	0.16 μM	cells	[3]
Uranine	Chemiluminescence	2-1000 μM	2.00 μM	Tap water	[4]
nanoflare	Fluorescence	50-1000 nM	8.51 nM	living cells	[5]
Au/Ag alloy NPs	Colorimetry	2.40-24.00 μM	0.30 μM	Water	[6]
SQDs/AgNPs	Fluorescence	0.1 - 100 μM	0.08 μM	Water	[7]
Eu_2O_3/BPQDs	Chemiluminescence	1 - 1000 μM	0.20 μM	$PM_{2.5}$	This work

Table S2. Comparisons of proposed method with recently reported strategies for Ti^{4+} detection.

Detection probe	methods	Linear range	LOD	Samples	Reference
CS_2	Raman	----	0.020 μM	$TiCl_4/CH_2Cl_2$	[8]
---	TLC-spectrophotometry	12-62.7 μM	----	bauxite	[9]
---	EAAS	7.92-31.8 μg/gm	---	human tissues	[10]
Eu_2O_3/BPQDs	Chemiluminescence	0.02 - 83 μM	0.005 μM	$PM_{2.5}$	This work

References

[1] B. Zhu, W. Tang, Y. Ren and X. Duan, *Anal. Chem.*, 2018, **90**, 13714-13722.

[2] T. Dutta, F. Chandra and A. L. Koner, *Spectrochim. Acta A: Mol. Biomol. Spectrosc.*, 2018, **191**, 217-220.

[3] Y. Dai, Z. Zhan, L. Chai, L. Zhang, Q. Guo, K. Zhang and Y. Lv, *Anal. Chem.*, 2021, **93**, 4628-4634

[4] T. Y. M. H. Nakagama, *Anal. Chim. Acta.*, 1990, **231**, 7-12.

[5] K. Wu, C. Yao, D. Yang and D. Liu, *Biosens. Bioelectron.*, 2022, **209**, 114273

[6] K. I. M. Shanmugaraj, *New J. Chem.*, 2017, **41**, 14130-14136.

[7] L. Liu, G. Zhu, W. Zeng, B. Lv and Y. Yi, *Anal. Bioanal. Chem.*, 2019, **411**, 1561-1568.

[8] X. Xiang, X. He, W. Xia, J. Yin, X. Yuan and X. Zhou, *Anal. Methods-UK*, 2020, **12**, 988-995.

[9] J. J. U. R. Mohamed Najar P A, *Chin. J. Chromatogr.,* 2005, **23**, 555-561.

[10] M. D. M. H. Daniel S. Jorgenson, *Plast. Reconstr Surg.*, 1997, **99**, 976-979.